J. Ind. Geophys. Union, 30(1) (2026), 35-44
https://doi.org/10.71122/JIGU.30(1)2026.004

Seismic site characterization in the region near Korba coalfield, Chhattisgarh (India)

Tushar Singhania[1,2], Niptika Jana[1*] and Sanjit Kumar Pal[1]
[1]Department of Applied Geophysics, Indian Institute of Technology (Indian School of Mines)
Dhanbad, Dhanbad-826004, Jharkhand, India
[2]Department of Civil and Infrastructure Engineering, Indian Institute of Technology Jodhpur, Jodhpur District-342030, Rajasthan, India
**Corresponding author: niptika.jana.1201@gmail.com*

ABSTRACT

This study employs seismic techniques for the site characterization of the Korba region in Chhattisgarh, India. Seismic activity has been reported in this region lately, classifying this region in seismic zone III, according to the Building Materials and Technology Promotion Council (BMTPC) assessment (2006). We gather data from 30 different locations in the Korba region, using the Tromino instrument. We estimate the fundamental frequency, construct shear wave velocity for subsurface classification of the Korba region, and develop Horizontal-to-Vertical Spectral Ratio (HVSR) curves for ambient noise data in accordance with the National Earthquake Hazards Reduction Programme (NEHRP) criteria. We calculated the liquefaction vulnerability index (Kg), amplification value, and peak resonant frequencies from the HVSR curve. Amplification factors range from 1.18 to 10.02, while the peak resonant frequencies span from 1.146 to 15.062 Hz. Vs30 for the region varies between 140.06 and 646.90 m/s. These findings indicate presence of soft soil in the western portion of the region, which is situated along the Hasdeo River's bank. In majority of the places, we discovered that the Kg value was less than 10, indicating low liquefaction vulnerability in the examined area.

Keywords: Horizontal-to-vertical spectrum (HVSR), Shear wave velocity, Peak resonant frequency, Site characterization, Liquefaction vulnerability index (Kg), Digital Elevation Model (DEM).

INTRODUCTION

Classification of the nature of subsurface, plays a major role in generating seismic damage risks (Gupta et al. 2021), as soil properties influence the likelihood and severity of an earthquake in a particular region (Akkaya and Ozvan, 2019). Earthquakes produce strong and dynamic forces that travel through the earth as seismic waves. These waves have the potential to induce seismic activity, resulting in vibrations that can impact structures and their foundations. Comprehending the soil's response to these dynamic stresses, is crucial as it differs significantly from its behaviour under static loads, such as the weight of a structure (Farrugia et al., 2016). Understanding the behaviour of soil under dynamic loads, helps in selecting suitable structures that can withstand seismic forces and implementation of appropriate mitigation measures. The soft soil layer's resonance frequency and shear wave velocities (V_S), are crucial for predicting ground motion and effectively preventing or mitigating seismic catastrophes (Farrugia et al., 2016). Comprehending the geographical variances is crucial for evaluating earthquake hazards, preparing for them, and designing robust infrastructure (Ansal, 1999).

Many studies have been conducted on seismic site characterization in various regions (Picozzi et al., 2009; Foti et al., 2011; Gupta et al., 2019; Cultrera et al., 2021; Gupta et al., 2021; Vijayan et al., 2022). However, no similar study has been conducted in the surrounding areas of the Korba region. The current increase in seismic activity in several districts of Chhattisgarh, including Korba, highlights the need to understand the subsurface dynamics for upcoming developmental projects (Parashar, 2023).

The studied region lies under seismic zone 'III' of India, which is a moderate-intensity zone that is assigned under zone factor 0.16. (BMTPC 2nd edition). The Hasdeo river flows in the southern part of the Korba, which divides it into two parts (Singh et al., 2016). The coal mines of Korba include Manikpur, Gevra, Dipka, Kusumunda, Laxman, Pavan, Rajgamar, Balig, Banki, and Surakachhar, out of which Manikpur, Gevra, Dipka and Kusumunda are operated as open cast mines (Singh et al., 2016).

The current population of the Korba region is approximately 5,00,000, which has increased by 1.86% since 2022 (Census of India, 2011). With the increase in population, more construction work is happening in this region. The Korba region lies in seismic zone III, where an earthquake up to magnitude 6 can be expected (Sairam et al., 2011). This would have the potential to damage single-story or multi-story buildings. Therefore, any development in this region should be done by taking into consideration the seismic parameters to mitigate potential damages and ensure resilient development of projects.

Seismic site characterization is often used to identify the sub-surface material properties of the earth. Parameters that are used to define these material properties are, the shear modulus and shear wave velocity, among others (Pandey et al., 2016). Vs 30 value varies with depth as the subsurface profile changes, so thereby with the application of site characterization, we can identify the material properties of any zones as well (Gupta et al., 2019). Many site characterisation techniques are used to identify the characteristics of a site to facilitate ground response analysis, such as Horizontal-to-vertical spectral ratio (HVSR) (Nakamura, 1989), Multichannel analysis of surface wave (MASW) (Park et al., 1999), Surface analysis of surface waves (SASW), and many more.

In the current study, the Horizontal to Vertical spectral ratio (HVSR) site characterization method was used to classify the subsurface characteristics in the Korba region. Because of its affordability and ease of integration, HVSR is one of the popular non-invasive geophysical site characterization technique, which is used for the measurement of site amplification through the resonant frequency, generated by a three-component seismograph (Lachetl and Bard, 1994). After Nakamura (1989), many researchers used this technique to analyse the seismic site characterization (Nakamura, 1989, 1996, 2000; Field and Jacob, 1993; Bard, 1998; Gallipoli and Mucciarelli, 2009; Sisman et al., 2018; Tiwari et al., 2024). The main objective of this study is to generate the HVSR curves for ambient noise data and estimate the predominant frequency, i.e., fundamental frequency. Then, further inverting the data, we aim to achieve the shear wave velocity profiles to classify the sub-surface of the Korba region as per National Earthquake Hazards Reduction Program NEHRP guidelines (Safety, 2003). The NEHRP, classifies the soil into five types based on their average shear wave velocity at 30 m (Vs30), i.e.,

(i) Soil Type A: Vs30 > 1500m/s, described as hard rock.

(ii) Soil Type B: 760<Vs30< 1500m/s, described as rock.

(iii) Soil Type C: 360<Vs30< 760m/s, described as soft rock/very stiff soil, mostly gravels.

(iv) Soil Type D: 180<Vs30< 360m/s, described as sand, silt, very stiff clay or some gravels.

(v) Soil Type E: Vs30< 180m/s, described as soft clay.

For this purpose, we attempted to collect ambient noise data by using the Tromino instrument in the Korba region. The Tromino is a versatile all-in-one seismometer used for subsoil characterization (HVSR, MASW, and more) and vibration monitoring. It is equipped with three velocimetric and accelerometric channels, one analog channel, and one GPS receiver. Its working range is 0.1Hz to 1024 Hz, making it a valuable tool for a wide range of seismic studies. (https://www.tromino.it/). The HVSR curves are used to measure the velocity contrast between the upper and the lower sedimentary layer of the earth (Parolai et al., 2002)

GEOLOGY AND TECTONICS

The study area covers the region between 22°15′ N to 22°30′ N and 82°15′ E to 82°55′ E with an area of about 530 km^2 (Raja Rao, 1983). Singh et al. (2016) reported some of the operational mines in the Korba region, which include Gevra, Dipka, Kusumunda, Manikpur and Rajgamar. One of the study (Govil and Guha 2023) reported the lithology of the Rajgamar coal mine, where they described the occurrence of an alluvial soil layer within the top 5.2 m of the ground. beneath that there are different layers of sandstone, coal, shale sandstone, seam coal and coal. Singh et al. (2016) further showed that the Gondwana rocks occur all around the Korba coalfield except on the east side where Archean rocks are present, besides Barakars, Talchirs and Kamthi formations. The southern part of the Korba coalfield is faulted, due to which the upper part of the Barakar formation is directly exposed over the underlying basement.

In another significant study, Singh et al. (2018), which focused on a region primarily distinguished by the upper strata of the Early Permian Barakar Formation, belonging to the Lower Gondwana Group. The geological formations in this region have an east-west orientation and often have a southerly inclination of around 5°-8°. The region is characterised by many transverse faults that exhibit varied orientations, including northeast-southwest, northwest-southeast, and east-west, with varying levels of displacement. An east-west fault is also located which tilts towards the south and connects the Upper and Lower Barakar Formations. Significantly, this geological fault separates the Lower Barakar Formation from the Upper Barakar Formation and probably intersects the Hasdeo River with a very small amount of displacement. The E-W trending fault is the primary structural feature in the area and serves as a major source of seismic activity. It influences the subsurface hydrology and can trigger minor seismic events.

METHODOLOGY

Horizontal to vertical spectral ratio (HVSR)

Nakamura (1989), though credited as the developer of this technique, it was originally suggested by Nogoshi and Igarashi (1970). The fundamental frequency of the soil and site amplification from microtremor data are estimated using the HVSR method. This method helps construction engineers to implement earthquake-resistant design features. It increases resilience and safety. It also improves earthquake preparedness and reduces potential damage during future seismic events. Weak and strong ground motions can be used to construct HVSR curves for soil characterisation (Gallipoli and Mucciarelli, 2009; Özalaybey et al., 2011; Askan et al., 2015, 2017; Sisman et al., 2018; Gupta et al., 2019). HVSR determines the amount of signal strength variation across various frequencies in both horizontal and vertical directions. It’s a mean of comprehending a signal’s properties in terms of its directed energy distribution. It is defined as,

$$HVSR = \frac{\sqrt{H_{NS}^2 + H_{EW}^2}}{V} \tag{1}$$

Where the vertical, east-west, and north-south components of the waveform are denoted by V, H_{EW}, and H_{NS}, respectively.

The distinctive shape of the HVSR amplitude offers a dependable estimate of the site amplification function. This function contributes significantly to the resonance effect, significantly contributing to heightened vibrations within a structure (Nakamura, 1989; Lachetl and Bard, 1994; Herak, 2008; Clavero et al., 2014). Our method carefully follows the steps and guidelines provided by SESAME (2004) for the collection and processing of ambient noise data for HVSR calculation.

Data acquisition and processing

This study used a Tromino instrument to collect microtremor data from 30 observation points in the studied region as shown in **Figure 1**. The Tromino instrument features three-component orthogonal velocity meters, susceptible to electrodynamic signals. As directed by the instructions of the manufacturer's, the Tromino is positioned and levelled on flat ground, aligned north-south to capture noise data (Gupta et al., 2019, 2021). According to Okada and Suto (2003), frequencies more than 1 Hz are produced by anthropogenic sources, while frequencies lower than ~1 Hz are often associated with natural events. The microtremor data was gathered for 30 minutes at a sample frequency of 1024 Hz at each observation site. HVSR data processing was done using Geopsy software (www.geopsy.org).

Additionally, the data was processed by dividing them into stationary windows of 20 to 40 seconds, with the following parameters applied: 2s for short-term averaging (STA), 30s for long-term averaging (LTA), and 0.2 and 0.3s for low and high STA/LTA thresholds, respectively (Hellel et al., 2012). The individual spectra were processed using the technique of Konno and Ohmachi (1998) with a bandwidth coefficient of b=40, before being averaged. Following the widely accepted standard criteria described in SESAME (2004), a demonstration of Horizontal-to-Vertical Spectral Ratio (HVSR) curve was calculated for every site and those in the array. The liquefaction vulnerability index (K_g) values at each location were determined through an empirical formula correlating the dominant frequency (f_o) and amplification factor (A_o).

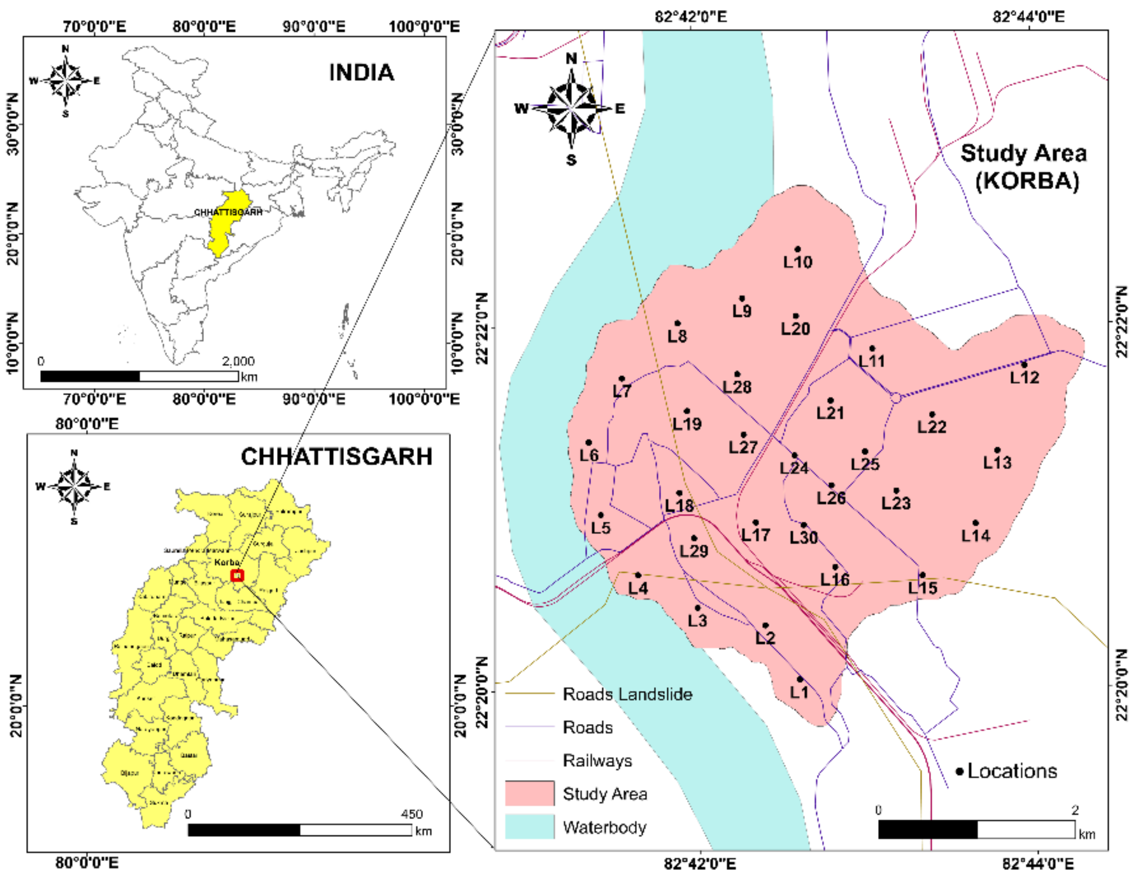

Figure 1. Map showing the locations of microtremor area measurement

$$K_g = \frac{A_O^2}{f_O} \quad (2)$$

Shear wave velocity

The Dinver software (www.geopsy.org) was used for the inversion of the HVSR curve, resulting in the velocity profile for the input data. The inversion process involves systematically searching for parameters that yield the optimal model by minimizing the misfit value (Hobiger, 2011). Parameter constraints that were applied in Dinver during the inversion are, compression-wave velocity, Poisson's ratio, shear-wave velocity, and density. All the parameters were defined as per the pre-defined specified ranges. P wave velocity (Vp), S wave velocity (Vs), and density characteristics were employed as limitations in previous studies to create a model that closely approximates the actual subsurface structure (Katriani et al., 2019; Susilanto et al., 2019). The ellipticity curve is a useful modelling tool that is utilised in the inversion of the HVSR curve. The idea behind this method is to combine the signal window derived from microtremor data in order to distinguish Rayleigh waves from other types of waves. The energy of the combined horizontal and vertical signals inside the signal window is then calculated beyond that. The ellipticity of Rayleigh waves may be determined using this energy as a measure. A relationship between the subsurface structure and the Rayleigh wave ellipticity is established and is explained as a function of frequency. In particular, it sheds light on the sediment thickness and shear wave velocity profiles within the geological layers. Essentially, by carefully examining the Rayleigh wave properties, the ellipticity curve becomes an invaluable instrument for understanding the complex features of underground structures (Hobiger et al., 2009).

RESULTS AND DISCUSSION

For 30 investigated sites in the Korba region, the Horizontal-to-Vertical Spectral Ratio (HVSR) curves were obtained. Examples of the HVSR curves of some investigated locations are shown in Figure 2. This showed the dominant frequency and amplitude characteristics, which are shown in Figures 3 and 4, respectively. The presented spectral ratios showed a frequency range of 0.2-20 Hz, which is essential for assessing common civil engineering structures. Impedance differences between the underlying hard rock and the superficial soft layers are indicated by diagnostic peaks in the HVSR curves. Large peak values frequently indicate sharp contrasts, which may imply that ground motion is amplified (Parolai et al., 2002; Sukumaran et al., 2011; Singh, 2015; Singh et al., 2017a).

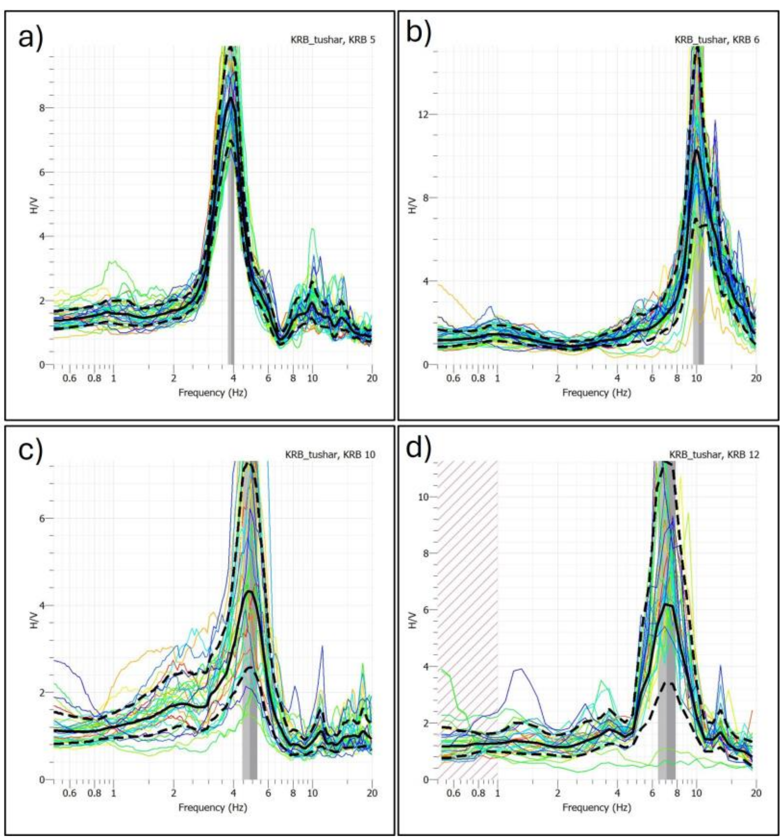

Figure 2. A sample of HVSR curves obtained at **(a)** location 5 (Sarwamangala Para), **(b)** location 6 (Ratakhar), **(c)** location 10 (Dhondi Para) and **(d)** location 12 (Manglam Vihar).

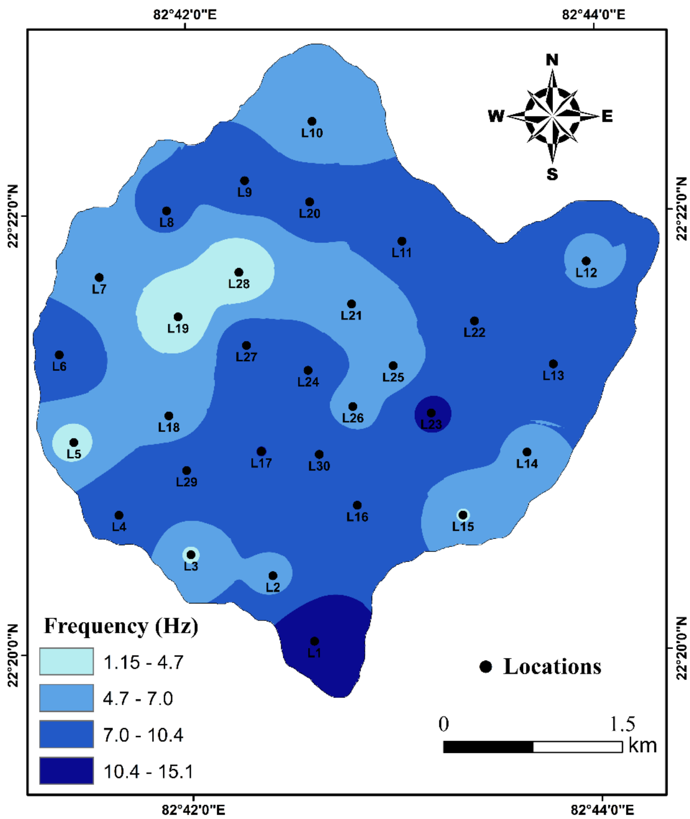

Figure 3. Spatial distribution of peak resonant frequency (Hz) in the study area. Black dots indicate the locations of measurement points.

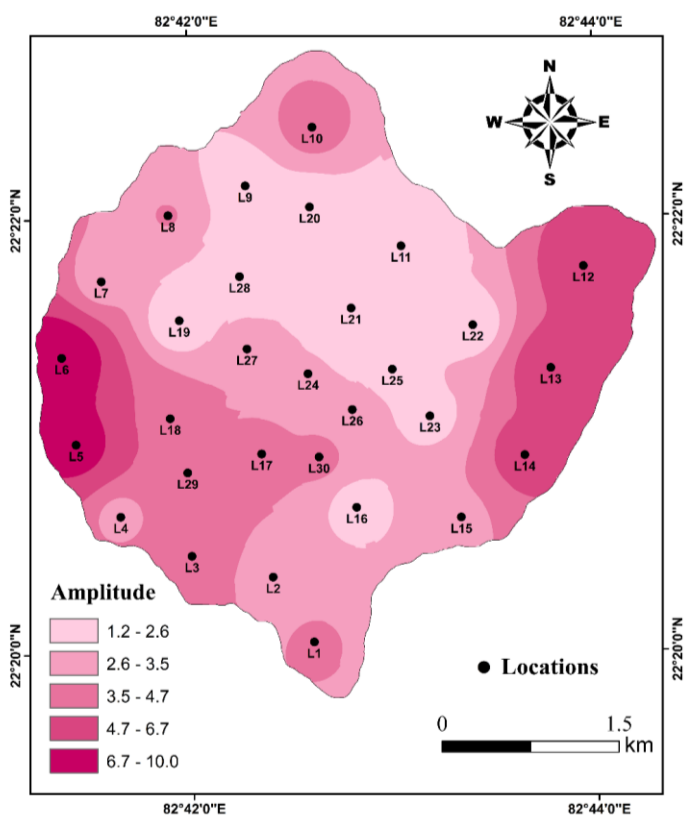

Figure 4. Spatial distribution of amplification factor in the study area. Black dots indicate the locations of measurement points.

Peak resonant frequencies in the Korba region vary mostly between 1.146 and 15.062 Hz, and the corresponding amplification factors fall between 1.18 and 10.02. Figure 5 represents some examples of shear wave velocity profiles at a depth of 30 m (Vs30), as derived by the inversion of HVSR curves. The value of Vs30 ranges from 140.06 to 646.90 m/sec.

Our results indicate that the majority of the Korba region under study fits into the D soil type category, which can be defined as sand, silt, extremely stiff clay, or certain gravels, in accordance with the guidelines of the NEHRP, as can also be noted from Figure 6.

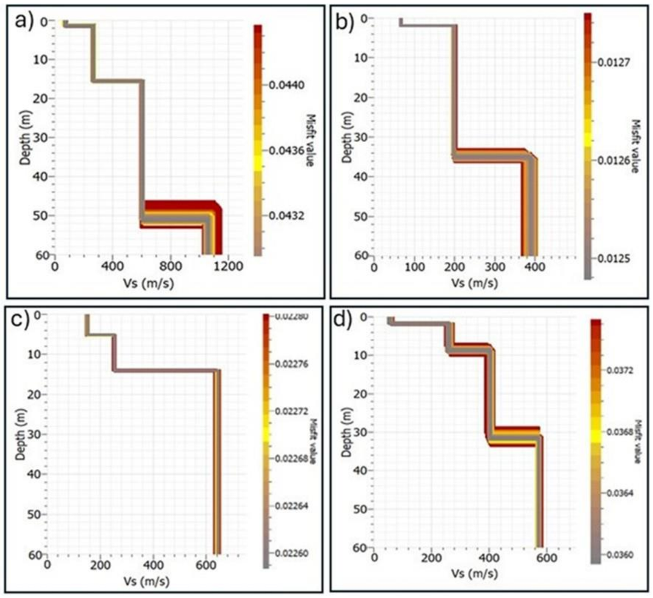

Figure 5. A sample of shear wave velocity profiles obtained at **(a)** location 5 (Sarwamangala Para), **(b)** location 6 (Ratakhar), **(c)** location 10 (Dhondi Para) and **(d)** location 12 (Manglam Vihar).

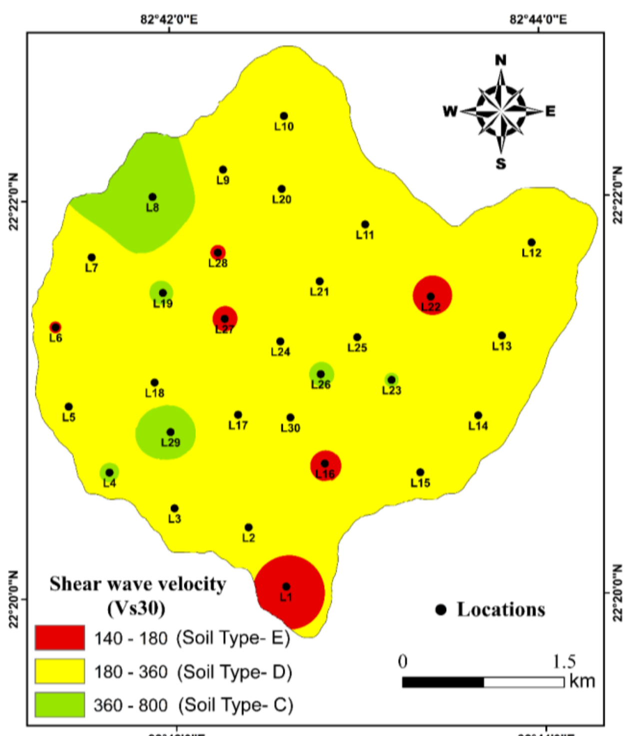

Figure 6. Spatial distribution of shear wave velocity (Vs30) in the study area. Black dots indicate the locations of measurement points

In the western part of the region located to the bank side of the Hasdeo River, the value of amplification factor and peak resonant frequency was observed to be relatively high and low, respectively, which indicates that the soil in that part would be less denser or near to soft (Kramer, 1996). In the North- Eastern part of the study area, the value of the amplitude and peak resonant frequency was observed to be relatively low and high, respectively, which indicates that the soil in that part would be more denser or soft rock (Kramer, 1996). Figure 7 illustrates the Digital Elevation Model (DEM, i.e., Cartosat DEM of 30 m resolution, revealing a distinct topographical pattern along the Hasdeo riverbank. To the west of the region, the terrain exhibits lower elevations, gradually ascending towards the east. Furthermore, the amplitude and frequency values indicate a correlation with soil density. Softer soil can be observed in the lower elevation areas, while denser soil is prevalent in the higher elevation regions.

Further, the soil's vulnerability to liquefication was measured using the liquefaction vulnerability index (K_g value) (Nakamura, 1996). For the betterment of land use planning and mitigating the risk of earthquakes, K_g values offer crucial information on the site's condition (Singh et al., 2017b). The K_g value ranges from 0.03 to 17.65, as seen in Figure 8. High K_g values were found at two locations along the Hasdeo River, indicating that liquefaction occurs at areas with Kg > 10 during large earthquakes (Nakamura, 1996; Huang and Tseng, 2002; Saita et al., 2004; Beroya et al., 2009; Singh et al., 2017b). The K_g value in this study appears to be lower, suggesting that the investigated Korba regions have a lower risk of damage from liquefaction (Singh et al., 2017a).

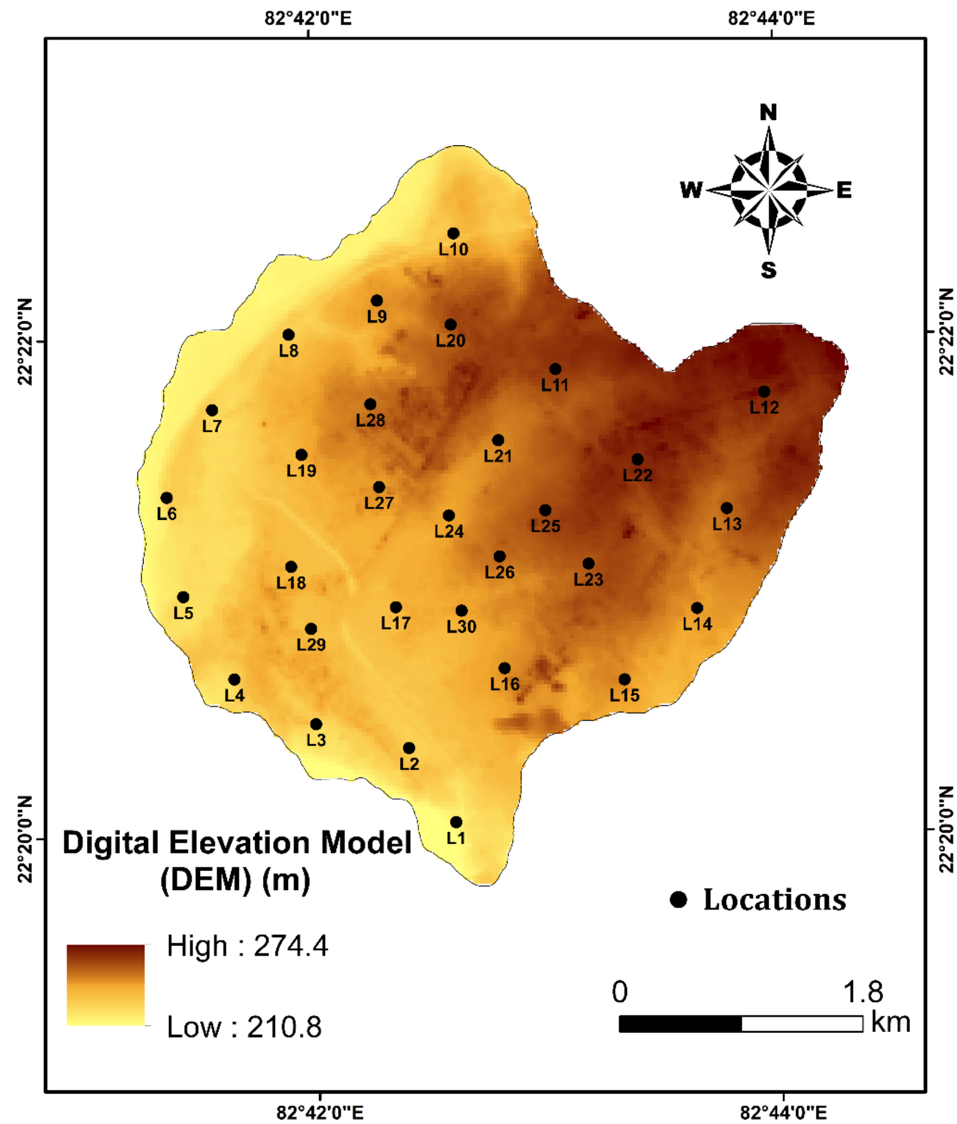

Figure 7. Digital Elevation Model (DEM) for the study area. Black dots indicate the locations of measurement points

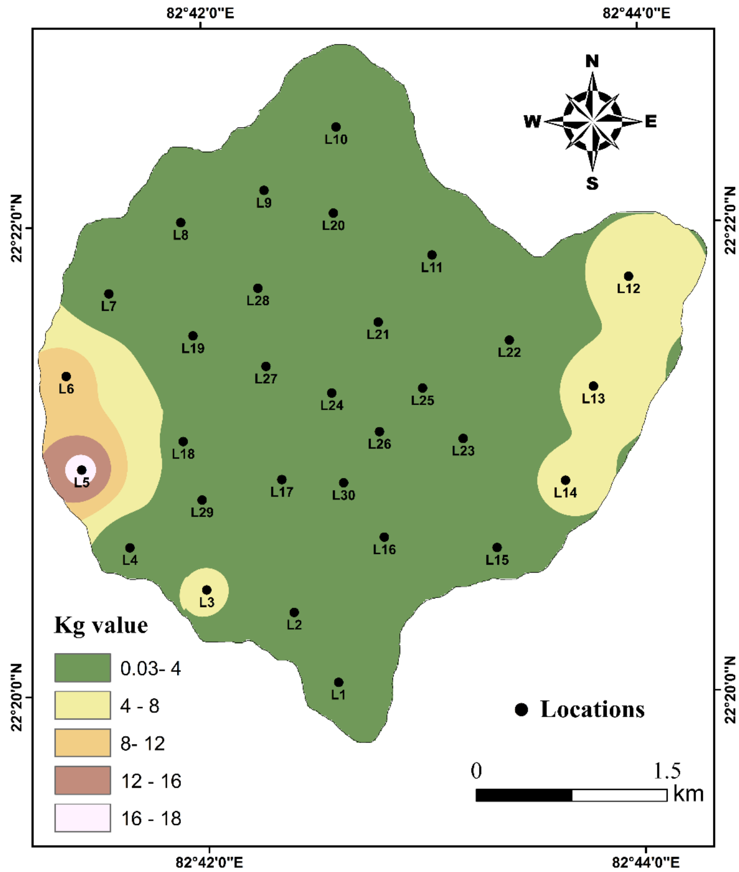

Figure 8. Spatial distribution of Liquefaction Vulnerability Index (Kg) for the study area. Black dots indicate the locations of measurement points

CONCLUSIONS

In the present study, we examined the ambient noise data for 30 sites in the Korba area. Our primary objectives was to provide liquefaction vulnerability index (Kg), shear wave velocity (Vs30) profile, and horizontal-to-vertical spectral ratio (HVSR) curves. Our findings reports the presence of soft soil in the western part of the studied region, which means that these areas are more prone to liquefaction. Our findings in this study will help the engineers to consider all the important factors required before conducting any construction projects in that region. We also find that in the major part of the studied region, the value of the liquefaction vulnerability index is very low, which indicates that these areas have a low risk of ground failure and damage to infrastructure due to low liquefaction during earthquakes, which has important implications for planning of construction projects and disaster preparedness efforts.

Acknowledgement

Tushar Singhania expresses gratitude to Akash Rajput for the help extended during the data collection. Further gratitude is also expressed to Amit Bera for his support in the geoprocessing stages, facilitating an understanding of the instrument and software. No funding agency has given a particular grant for this project. The institutional and national research committees' ethical criteria were followed in every procedure carried out for this investigation.

Author Credit Statement

Tushar Singhania is credited with the data collection, data processing, interpretation and drafting of the manuscript. Niptika Jana is credited with study formation, interpretation, drafting and review of the manuscript. Sanjit Kumar Pal is credited with instrumentation support and review.

Data availability

Data can be made available on a reasonable request.

Compliance with Ethical Standards

The authors declare no conflict of interest and adhere to copyright norms.

REFERENCES

Akkaya, I. and Ozvan, A., 2019. Site characterization in the Van settlement (Eastern Turkey) using surface waves and HVSR microtremor methods. J. Appl. Geophys., 160, 157–170.

Ansal, A.M., 1999. Strong ground motions and site amplification. Earthquake Geotechnical Engineering, 2, 879–894.

Askan, A., Ansal, A., Kurtuluş, A., Kutanis, M., Sucuoglu, H. and Bakir, S., 2015. Assessment of seismic hazard in the Erzincan (Turkey) region: construction of local velocity models and evaluation of potential ground motions. Turk. J. Earth Sci., 24(6), 529–565.

Askan, A., Ansal, A., Kurtuluş, A. and Erdik, M., 2017. An interdisciplinary approach for regional seismic damage estimation. Proc. 16th World Conference on Earthquake Engineering, Santiago, Chile, Jan. 9–13.

Bard, P., 1998. Microtremor measurements: a tool for site effect estimation. In Proceedings, The Effects of Surface Geology on Seismic Motion, 3, 1251–1279.

Beroya, M.A.A., Bautista, M.L.P., Narra, J.C. and Orense, R.P., 2009. Use of microtremor in liquefaction hazard mapping. Eng. Geol., 107(3–4), 140–153.

Building Materials & Technology Promotion Council, Government of India, 2006. Vulnerability Atlas of India, 2nd ed.

Census of India, 2011: Provisional Population Totals. Government of India, 409–413.

Clavero, D., Molina, S., Alarcon, A. and Ruiz, A., 2014. Shear wave velocity estimation in the metropolitan area of Málaga (S Spain). J. Appl. Geophys., 109, 175–185.

Cultrera, G., Cornou, C., Di Giulio, G. and Bard, P.Y., 2021. Indicators for site characterization at seismic stations: recommendations from a dedicated survey. Bull. Earthq. Eng., 19(11), 4171–4195.

Farrugia, D., Paolucci, E., D'Amico, S. and Galea, P., 2016. Inversion of surface wave data for subsurface shear wave velocity profiles characterized by a thick buried low-velocity layer. Geophys. J. Int., 206(2), 1221–1231.

Field, E. and Jacob, K., 1993. The theoretical response of sedimentary layers to ambient seismic noise. Geophys. Res. Lett., 20(24), 2925–2928.

Foti, S., Parolai, S., Albarello, D. and Picozzi, M., 2011. Application of surface-wave methods for seismic site characterization. Surv. Geophys., 32, 777–825.

Gallipoli, M.R. and Mucciarelli, M., 2009. Comparison of site classification from Vs30, Vs10, and HVSR in Italy. Bull. Seismol. Soc. Am., 99(1), 340–351.

Govil, H. and Guha, S., 2023. Underground mine deformation monitoring using synthetic aperture radar technique: a case study of Rajgamar coal mine, Korba, Chhattisgarh, India. J. Appl. Geophys., 209, 104899.

Gupta, R.K., Mahajan, A.K. and Shukla, K., 2019. Site characterization through combined analysis of seismic and electrical resistivity data at Dhanbad, Jharkhand, India. Environ. Earth Sci., 78(6), 226.

Gupta, R.K., Mahajan, A.K., Mittal, H. and Bhattacharya, S.N., 2021. Seismic site characterization and site response study of Nirsa (India). Nat. Hazards, 108(2), 2033–2057.

Hellel, M., Roubion, C., Bensalem, R. and Bard, P.Y., 2012. Basement mapping with single-station and array ambient vibration data: delineating faults under Boumerdes City, Algeria. Seismol. Res. Lett., 83(5), 798–805.

Herak, M., 2008. ModelHVSR- A Matlab tool to model horizontal-to-vertical spectral ratio of ambient noise. Comput. Geosci., 34(11), 1514–1526.

Hobiger, M., 2011. Polarization of surface waves: characterization, inversion and application to seismic hazard assessment. PhD Thesis, Université de Grenoble.

Hobiger, M., Bard, P.Y., Fäh, D. and Scherbaum, F., 2009. Single station determination of Rayleigh wave ellipticity by using the random decrement technique (RayDec). Geophys. Res. Lett., 36(14), L14303.

Huang, H.-C. and Tseng, Y.-S., 2002. Characteristics of soil liquefaction using H/V of microtremors in Yuan-Lin area, Taiwan. Terr. Atmos. Ocean. Sci., 13(3), 325–338.

Katriani, L., Daryono, M.R., Prasetya, G. and Susilanto, P., 2019. Identification of subsurface lithology in Sendang Mulyo, Purwoharjo Village, Samigaluh Subdistrict, Kulon Progo Regency. J. Phys. Conf. Ser., 012008.

Konno, K. and Ohmachi, T., 1998. Ground-motion characteristics estimated from spectral ratio between horizontal and vertical components of microtremor. Bull. Seism. Soc. America, 88(1), pp.228-241.

Kramer, S.L., 1996. Geotechnical Earthquake Engineering. Pearson Education India.

Lachetl, C. and Bard, P.Y., 1994. Numerical and theoretical investigations on the possibilities and limitations of Nakamura's technique. J. Phys. Earth, 42(5), 377–397.

Nakamura, Y., 1989. A method for dynamic characteristics estimation of subsurface using microtremor on the ground surface. Railw. Tech. Res. Inst. Q. Rep., 30(1), 25–33.

Nakamura, Y., 1996. Real-time information systems for seismic hazard mitigation: UrEDAS, HERAS and PIC. Q. Rep. RTRI., 37(3), 112–127.

Nakamura, Y., 2000. Clear identification of fundamental idea of Nakamura's technique and its applications. Proc. 12th World Conference on Earthquake Engineering, 2656, 1–8.

Nogoshi, M. and Igarashi, T., 1970. On the propagation characteristics of microtremors. J. Seism. Soc. Japan, 23, pp.264-280.

Okada, H. and Suto, K., 2003. The microtremor survey method. Soc. Expl. Geophysicists.

Ozalaybey, S., Zor, E., Erdik, M., Alptekin, O., Tapirdamaz, M.C. and Yılmaz, Y., 2011.

Investigation of 3-D basin structures in the Izmit Bay area (Turkey) by single-station microtremor and gravimetric methods. Geophys. J. Int., 186(2), 883–894.

Pandey, B., Jakka, R.S., Kumar, A. and Mittal, H., 2016. Site characterization of strong-motion recording stations of Delhi using joint inversion of phase velocity dispersion and H/V curve. Bull. Seismol. Soc. Am., 106(3), 1254–1266.

Parashar, A.K., 2023. A seismic hazard assessment of North Chhattisgarh (India).. Natural Hazards: New Insights. p. 35

Park, C.B., Miller, R.D. and Xia, J., 1999. Multichannel analysis of surface waves. Geophysics, 64(3), 800–808.

Parolai, S., Bormann, P. and Milkereit, C., 2002. New relationships between Vs, thickness of sediments, and resonance frequency calculated by the H/V ratio of seismic noise for the Cologne area (Germany). Bull. Seismol. Soc. Am., 92(6), 2521–2527.

Picozzi, M., Strollo, A., Parolai, S., Durukal, E., Ozel, O., Karabulut, S., Zschau, J. and Erdik, M., 2009. Site characterization by seismic noise in Istanbul, Turkey. Soil Dyn. Earthq. Eng., 29(3), 469–482.

Raja Rao, C.S., 1983. Coalfields of India Vol. III: Coal Resources of Madhya Pradesh and Jammu and Kashmir. Bull. Geol. Surv. India Ser. A, 45, 204.

Safety, I.S., 2003. NEHRP recommended provisions for seismic regulations for new buildings and other structures (FEMA 450).

Sairam, B., Rastogi, B.K., Aggarwal, S., Chauhan, M. and Bhonde, U., 2011. Seismic site characterization using Vs30 and site amplification in Gandhinagar region, Gujarat, India. Curr. Sci., 754–761.

Saita, J., Bautista, M.L.P. and Nakamura, Y., 2004. On relationship between the estimated strong motion characteristics of surface layer and earthquake damage—case study at Intramuros, Metro Manila. Proc. 13th World Conference on Earthquake Engineering, 1–7.

SESAME, 2004. Guidelines for the implementation of the H/V spectral ratio technique on ambient vibrations measurements, processing and interpretation. European Commission–EVG1-CT-2000-00026 SESAME, 1–62.

Singh, A.K., Varma, N.P. and Mondal, G.C., 2016. Hydrogeochemical investigation and quality assessment of mine water resources in the Korba coalfield, India. Arab. J. Geosci., 9, 1–20.

Singh, A.P., 2015. Seismic hazard evaluation in Anjar city area of western India: microtremor array measurement. Soil Dyn. Earthq. Eng., 71, 143–150.

Singh, A.P., Mishra, O.P., Kumar, A., 2017a. Characterizing surface geology, liquefaction potential, and maximum intensity in the Kachchh seismic zone, Western India, through microtremor analysis. Bull. Seismol. Soc. Am., 107(3), 1277–1292.

Singh, A.P., Parmar, A. and Chopra, S., 2017b. Microtremor study for evaluating the site response characteristics in the Surat City of western India. Nat. Hazards, 89(3), 1145–1166.

Singh, R., Venkatesh, A.S., Syed, T.H., Surinaidu, L., Pasupuleti, S., Rai, S.P. and Kumar, M., 2018. Stable isotope systematics and geochemical signatures constraining groundwater hydraulics in the mining environment of the Korba Coalfield, Central India. Environ. Earth Sci., 77, 1–17.

Sisman, F.N., Askan, A. and Asten, M., 2018. Evaluation of site response with alternative methods: a case study for engineering implications. Pure Appl. Geophys., 175(1), 257–273.

Sukumaran, P., Bhattacharya, S.N., Rai, S. and Mahajan, A.K., 2011. Profiling of late Tertiary–early Quaternary surface in the lower reaches of Narmada valley using microtremors. J. Asian Earth Sci., 41(3), 325–334.

Susilanto, P., Katriani, L., Daryono, M.R. and Prasetya, G., 2019. Analisis kecepatan gelombang geser (Vs) sebagai upaya mitigasi bencana gempabumi di Kulonprogo, DIY. J. Lingkung. dan Bencana Geol., 10(2), 45–53.

Tiwari, A., Rana, N. and Singh, G.P., 2024. A PGA amplification study for Varanasi city (India): Implications for seismic hazard assessment. J. Indian Geophys. Union, 28(6), 417-429.

Vijayan, A., Agrawal, M. and Gupta, R.K., 2022. Seismic site characterization using ambient noise and earthquake HVSR in the easternmost part of Shillong Plateau, India. J. Geol. Soc. India, 98(4), 471–478.

Received on: 17-01-25; Revised on: 6-11-2025; Accepted on : 12-11-2025